Pergamon

0301-9322(94)00077-8

Int. J. Multiphase Flow Vol. 21, No. 2, pp. 241–251, 1995

0301-9322/95 $9.50 + 0.00

STUDIES ON THE RELATIONSHIP BETWEEN THE STATISTICS OF VOID FRACTION FLUCTUATIONS AND THE PARAMETERS OF TWO-PHASE FLOWS†

R. KOZMA

Tohoku University, Department of Nuclear Engineering, Aramaki-Aza, Aoba, Sendai 980-77, Japan

(Received 17 May 1993; in revised form 13 October 1994)

Abstract—Based on Bernoulli statistics of bubble dynamics, a model of void fraction fluctuations in two-phase flows is introduced. The model is used to characterize changes of the intensity of void fraction fluctuations at various two-phase flow regimes, i.e. bubbly, slug and annular flows. Depending on the applied frequency band, the behavior of the band-passed variance of void fraction fluctuations changes significantly. At high frequencies, the band-passed variance increases monotonously with increasing void fractions, while the variance over the whole frequency range has a prominent maximum. By performing model calculations, the relationship between microscopic two-phase flow parameters and macroscopic flow quantities has been analyzed.

Key Words: void fraction fluctuations, Poisson variable, Bernoulli process, variance of void fraction

1. INTRODUCTION

During the past two decades, significant progress has been made in the identification of two-phase flow patterns by analyzing statistical properties of various measurement signals. The applied methods involve gamma- or X-ray transmission techniques, light-beam attenuation, pressure measurements, as well as experiments with local conductance probes. A detailed overview of these methods is given by Dukler & Taitel (1986). Air–water two-phase flow experiments by Jones & Zuber (1975), Lahey *et al.* (1978) and Vince & Lahey (1982) showed that the analysis of moments of the probability density function (pdf) of X-ray void-meter signals gives an insight into the structure of two-phase flows. Ohlmer *et al.* (1983) combined various measurement techniques for two-phase flow identification, using local conductance probes, pressure sensors and X-ray devices. Light-beam cross-correlation techniques have been applied by Lubbesmeyer & Leoni (1983). Power spectral density (PSD) and pdf of pressure signals have been used, e.g. by Jain & Roy (1983), Tutu (1984), Matsui (1986), Lin & Hanratty (1987) and Franca *et al.* (1991), to infer information about two-phase flow regimes.

In vertical two-phase flows, the following basic flow regimes can be defined: bubbly, slug, churn and annular. Bubbly and annular flows have unimodal character, i.e. their pdf is single-peaked. Slug flows are classified as bimodal and they have pdf with two peaks. The modality of the flow is related to the moments of the pdf. This relation has been investigated by Vince & Lahey (1982) in order to develop an objective flow regime indicator. They recommend the variance (2nd moment) of the pdf for flow regime identification. A relatively small variance value is the property of bubbly and annular flows, while slug flows have large variance. Bubbly-to-slug and slug-to-annular flow regime transitions manifest themselves through a sudden increase or decrease in the variance, respectively.

The present paper focuses on the relationship between the void fraction and the statistics of two-phase flows. According to Gaertner (1968) and Sultan & Judd (1978), the spatial distribution of bubble generation follows a Poisson law. By assuming that bubbles are produced as a Poisson process and they neither collapse nor coalesce while they pass through the channel with a constant

†Part of this work was carried out when the author was with the Delft University of Technology, IRI, Delft, The Netherlands.

velocity, a Poisson bubble statistics can be established. The Poisson statistics implies that distinct bubbles are uncorrelated (both in space and in time) and that the occurrence of bubbles is a rare event. The variance of the Poisson process is proportional to the probability of an event, i.e. bubble presence, in the control volume; see Jenkins & Watts (1968). Therefore, the variance of void fraction fluctuations is proportional to the actual void fraction in the case of Poisson model of void fraction fluctuations. Indeed, at low void fraction values, a linear relationship has been observed between the void fraction and the variance of void fraction fluctuations; see Vince & Lahey (1982).

The validity of the Poisson model breaks down at higher void fractions due to the following reasons. On the one hand, the occurrence of bubbles is not a rare event in bubbly flows with larger void fractions, when a lot of bubbles are found in the system and influence the detector signal simultaneously. On the other hand, the assumption of the Poisson model regarding the absence of temporal and spatial correlation between the bubbles is not valid in slug flows. Therefore, bubbles quickly forget the statistics of their birth and the bubble populations in the two-phase flow have clear non-Poissonian behavior. Consequently, there is a non-linear relationship between the void fraction and the variance of void fraction fluctuations.

Experimental evidence supports the conclusion that the Poisson bubble statistics are valid only at small void fraction values. According to Vince & Lahey (1982) and Matuszkiewicz *et al.* (1987), the variance of void fraction fluctuations has a maximum at a certain void fraction. Jain & Roy (1983) showed that the fraction of the high-frequency component of void fraction fluctuations increases monotonously with increasing void fractions. These effects can be explained by taking into account the presence of spatial and temporal correlations between bubbles in two-phase flows. In the interpretation, the following assumptions are used: (1) the two-phase flow is either unimodal or bimodal; (2) each mode has a unimodal pdf; (3) the pdf of the bimodal flow is the weighted sum of the pdfs of each mode, where the weights are the relative existence times of the modes; (4) the time-behavior of each mode has an oscillating character, i.e. the modes follow each other periodically. The quantitative characterization of the observed effects can be accomplished by means of a set of suitably chosen parameters. A successful characterization of two-phase flows is reported by Albrecht *et al.* (1984) by making use of five parameters (bubble velocity, void fraction of both modes, relative existence time of the modes and oscillation frequency).

In the present paper, the physical meaning of the parameters of non-Poissonian, bimodal two-phase flow models is investigated. It will be shown that the actual value of the variance of void fraction fluctuations is directly related to the size and distribution of bubbles in two-phase flows. Based on Bernoulli statistics of bubbles, the relationship between microscopic two-phase flow parameters and macroscopic statistical properties of void fraction fluctuations will be identified and analyzed.

2. BINOMIAL MODEL OF VOID FRACTION FLUCTUATIONS

2.1. General considerations

In this chapter, a model of void fraction fluctuations is introduced. We divide the void fraction signal into two components:

$$\epsilon(\mathbf{r}, t) = \bar{\epsilon}(\mathbf{r}) + \delta\epsilon(\mathbf{r}, t). \quad [1]$$

Here, $\epsilon(\mathbf{r}, t)$ is the actual value of the void fraction at position $\mathbf{r}$ and time t, $\bar{\epsilon}(\mathbf{r})$ is the average void fraction at $\mathbf{r}$. $\delta\epsilon(\mathbf{r}, t)$ is the time-dependent fluctuating component of the void fraction; the average value of $\delta\epsilon(\mathbf{r}, t)$ is zero. Let us Fourier-transform the fluctuating part of the void fraction:

$$\delta\epsilon(\mathbf{r}, \omega) = \mathscr{F}\{\delta\epsilon(\mathbf{r}, t)\}. \quad [2]$$

The auto power spectral density (APSD) of void fraction fluctuations will be calculated as follows:

$$\mathrm{APSD}_{\epsilon\epsilon}(\mathbf{r}, \omega) = \delta\epsilon(\mathbf{r}, \omega) \times \delta\epsilon^*(\mathbf{r}, \omega) \quad [3]$$

where * denotes the operation of complex conjugation. Depending on the actual void fraction model, different expressions of $\mathrm{APSD}_{\epsilon\epsilon}(\mathbf{r}, \omega)$ can be obtained.

A quantitative characterization of the noise intensity at a given frequency range is given by the normalized root-mean-square (NRMS) noise. The NRMS noise over frequencies f_1 to f_2 is defined as follows:

$$\mathrm{NRMS}_{\epsilon\epsilon}(\mathbf{r}_1, f_1, f_2) = \frac{1}{I}\sqrt{\int_{f_1}^{f_2} \mathrm{APSD}_{\epsilon\epsilon}(\mathbf{r}_1, f)\,\mathrm{d}f} \qquad [4]$$

Here I is the direct current (dc) component of the detector signal and f denotes frequency. In the case of $f_1 = 0$ and $f_2 \rightarrow f_{\max}$, the NRMS is equal to the normalized standard deviation of the pdf.

2.2. Bernoulli statistics of boiling noise

Let us consider a Bernoulli variable which takes values a and 0 with probabilities $P(a) = p$ and $P(0) = q = 1 - p$. By considering N independent Bernoulli variables, the possible sums of their outcomes are 0, a, $2a, \ldots, Na$. The probability distribution is binomial in the case of N events; see Jenkins & Watts (1968):

$$P(ka) = \binom{N}{k} p^k q^{N-k}; \quad k = 1, 2, \ldots, N. \qquad [5]$$

The mean μ_B and standard deviation σ_B of the binomial distribution are given by

$$\mu_B = Nap, \qquad [6]$$

$$\sigma_B = \sqrt{Na^2pq} \qquad [7]$$

Assume that the bubbles in a unit volume around spatial position $\mathbf{r}$ appear according to Bernoulli's law, with possible outcomes a (bubble is present) and 0 (absence of bubble). This means that bubbles appear independently in different space-time points. Here a denotes the unit change in the detector signal induced by a single bubble. Consider an observation volume which can accommodate maximum N bubbles (identical bubbles are considered). In the case of boiling monitoring by X-ray detectors, for example, this volume will be that part of the coolant channel which is illuminated by the X-ray beam. The probability of bubble appearance at a certain observation point $\mathbf{r}$ is the average local void fraction $\epsilon(\mathbf{r})$ which, in turn, can be identified as the parameter p of the Bernoulli process: $p = \epsilon(\mathbf{r})$.

According to our assumption about the absence of temporal-correlation between bubbles, the autospectrum of void fraction fluctuations in the unit observation volume does not depend on frequency. Its variance, $\sigma_B^2(\mathbf{r})$, is obtained from [7]:

$$\sigma_B^2(\mathbf{r}) = b_0^2\epsilon(\mathbf{r})(1 - \epsilon(\mathbf{r})) \qquad [8]$$

where $b_0^2 = Na^2$ does not depend on the void fraction. Similarly, the mean value of the void fraction fluctuations μ_B writes:

$$\mu_B = b_\epsilon \epsilon(\mathbf{r}) \qquad [9]$$

where $b_\epsilon = Na$. [8] indicates a parabolic relationship between the variance and ϵ instead of the linear dependence in the case of Poisson model. The physical meaning of coefficients b_0 and b_ϵ is given in the following discussions.

2.3. Bimodal void fraction fluctuation model

The assumption concerning spatial and temporal independence of bubbles is definitely not valid in slug flows, due to the presence of a well-defined spatial and temporal correlation in the void fraction fluctuation signal. Bubbly-to-slug flow regime transition takes place when the void fraction exceeds a threshold value. The value of the threshold can be estimated for known liquid and vapor volumetric fluxes. Part of the difficulties can be solved by introducing a modified binomial model, in which certain time-correlations are incorporated.

The modified model is based on the bimodal approximation of void fraction fluctuations in two-phase flows. The bimodal model is determined by the following set of parameters: μ_1 and μ_2, σ_1^2 and σ_2^2, which are the expected values and variances of the first and second mode, respectively. An additional parameter is the relative occurrence of mode 1, ϵ_L, where $0 \leqslant \epsilon \leqslant 1$. By making use of the above parameters, the following expressions can be obtained for the expected value μ_{BM} and variance σ^2_{BM} of the bimodal noise

$$\mu_{BM} = \epsilon_L \mu_1 + (1 - \epsilon_L)\mu_2 \quad [10]$$

$$\sigma^2_{BM} = \epsilon_L \sigma_1^2 + (1 - \epsilon_L)\sigma_2^2 + \epsilon_L(1 - \epsilon_L)(\mu_1 - \mu_2)^2 \quad [11]$$

The variance of the bimodal mixture is the sum of weighed variances of the separate modes and an additional term, which depends on the difference between the expected values of the two modes and on their relative frequency of occurrence (ϵ_L). For fixed μ_i and σ_i values, $i = 1, 2$, σ_{BM} is a quadratic function of ϵ_L with a maximum at position:

$$\epsilon_{L_{max}} = \frac{(\mu_1 - \mu_2)^2 + \sigma_1^2 - \sigma_2^2}{2(\mu_1 - \mu_2)^2} \quad [12]$$

If the parameters of the two modes are known *a priori*, the variance of the bimodal flow can be calculated from [11].

2.4. Relationship between microscopic two-phase flow parameters and measured void fraction characteristics

Let σ_1^2 and σ_2^2 be the variances of the two modes, both containing a background component ($\sigma^2_{i_{bg}}$) and a part induced by boiling ($\sigma^2_{i_{boil}}$):

$$\sigma_i^2 = \sigma^2_{i_{bg}} + \sigma^2_{i_{boil}}; \quad i = 1, 2. \quad [13]$$

Assume that the mean values and the variances of both modes satisfy [8] and [9], respectively. Then we obtain:

$$\mu_1 - \mu_2 = b_\epsilon(\epsilon_1 - \epsilon_2) \quad [14]$$

$$\sigma^2_{i_{boil}} = b_0^2 \epsilon_i (1 - \epsilon_i); \quad i = 1, 2 \quad [15]$$

Let us consider the physical meaning of b_ϵ and b_0.

- b_ϵ is equal to the ratio of the average value of the detector signal with full voidage in the observation volume and the value of the signal with zero void fraction. b_ϵ can be written in the form: $b_\epsilon = I(\epsilon = 0\%) - I(\epsilon = 100\%)$, where $I(\epsilon)$ denotes the value of the detector signal in case of void fraction ϵ. The value of b_ϵ can be determined by calculations and/or by measurements.
- b_0^2 is the void coefficient of the variance of void fraction fluctuations at $\epsilon = 0$, $b_0^2 = \partial\sigma_1^2/\partial\epsilon|_{\epsilon=0}$. b_0 can be either calculated on the basis of Poisson theory or it can be determined from measurements with low void fractions.

By taking into account [6] and[7], the following expressions are obtained for coefficients b_ϵ and b_0:

$$b_\epsilon = Na = I(\epsilon = 0\%) - I(\epsilon = 100\%) \quad [16]$$

$$b_0^2 = Na^2 = \partial\sigma_1^2/\partial\epsilon|_{\epsilon=0} \quad [17]$$

Here N is the maximum possible number of bubbles in the sensitivity volume of the detector; a is the absolute variation of the detector signal caused by a single bubble. For a known value of the maximum number and average size of bubbles, the extension of the sensitivity volume of the detector can be estimated and vice versa: a typical bubble size can be estimated for a given sensitivity volume. Based on [16] and [17], the maximum number of bubbles within the sensitivity volume of the detector writes:

$$N = b_\epsilon^2/b_0^2 \quad [18]$$

The above equation defines a relationship between the parameter N and measurable quantities b_0^2 and b_ϵ^2. In the forthcoming discussions, this relationship will be used to obtain information about the structure of two-phase flow.

2.5. Modeling σ^2 at different flow regimes

In this section, the description of the variance of void fraction fluctuations is given at different flow regimes. Bubbly-to-slug and slug-to-annular transitions will be analyzed, which are called type I and type II transitions, respectively. The variance of void fraction fluctuations in unimodal flows is described by [8]. Equation [11] describes σ^2 in bimodal flows. The void fraction ϵ of the bimodal flow satisfies the void balance equation:

$$\epsilon = \epsilon_L \sigma_1 + (1 - \sigma_L)\epsilon_2 \qquad [19]$$

Based on [19], ϵ_L can be expressed as a function of ϵ_1, ϵ_2 and ϵ:

$$\epsilon_L = \frac{\epsilon - \epsilon_2}{\epsilon_1 - \epsilon_2} \qquad [20]$$

By substituting [13], [14], [15] and [20] into [11], an expression is obtained for the variance in bimodal flows. This expression can be combined with the unimodal results to yield the general form of σ^2 for different flow regimes:

$$\sigma^2 = \begin{cases} Na^2\epsilon(1-\epsilon) + \sigma_0^2 & \text{if } \epsilon \leqslant \epsilon_{\mathrm{I}} \\ Na^2(\epsilon - \epsilon(\epsilon_1 + \epsilon_2) + \epsilon_1\epsilon_2) - N^2a^2(\epsilon^2 - \epsilon(\epsilon_1 + \epsilon_2) + \epsilon_1\epsilon_2) + \sigma_0^2 & \text{if } \epsilon_{\mathrm{I}} < \epsilon < \epsilon_{\mathrm{II}} \\ Na^2\epsilon(1-\epsilon) + \sigma_0^2 & \text{if } \epsilon_{\mathrm{II}} \leqslant \epsilon \end{cases} \qquad [21]$$

It is assumed that the background noise components of the two modes are equal: $\epsilon^2_{1;bg} = \sigma^2_{2;bg} = \sigma_0^2$. It is not the subject of the present study to investigate the dependence of flow regime maps on various two-phase flow parameters. For details of flow regime maps, see e.g. Taitel *et al.* (1980), Vince & Lahey (1982), McQuillan & Whalley (1985). Whenever it will be necessary in the model calculations, the following typical values of void fractions will be used: ϵ_{I} between 0.15 and 0.3, ϵ_{II} between 0.6 and 0.8, ϵ_1 from 0.1 to 0.4 and ϵ_2 from 0.5 and 0.8; see Dukler & Taitel (1986).

Results by Govier & Aziz (1972) and Jones & Zuber (1975) indicate that the bimodal system responds to void fraction changes first of all via the variation of the relative residence time of the two modes, while the variation of the properties of the modes is a second order effect. Therefore, first we consider ϵ_1 and ϵ_2 to be constant in a wide range of void fraction in bimodal flows. Later on, the effect caused by the variations of ϵ_1 and ϵ_2 will be studied as well.

According to [21], flow regime transitions appear in the form of jumps from one parabola to another. The two parabolas can be characterized as follows:

(1) The first parabola characterizes the behavior of σ^2 in bubbly ($\epsilon \leqslant \epsilon_{\mathrm{I}}$) and in annular ($\epsilon \leqslant \epsilon_{\mathrm{II}}$) flow regimes and it is symmetrical with respect to the $\epsilon = 0.5$ value. The coefficient of the quadratic term of this parabola is $-b_0^2$.

(2) The second parabola intersects the first one at points $\epsilon = \epsilon_1$ and $\epsilon = \epsilon_2$. The variances at these points are $\sigma_1^2 = b_0^2\epsilon_1(1 - \epsilon_1)$ and $\sigma_2^2 = b_0^2\sigma_2(1 - \epsilon_2)$, respectively. The second parabola describes bimodal slug flow: $\epsilon_{\mathrm{I}} \leqslant \epsilon \leqslant \epsilon_{\mathrm{II}}$. The coefficient of the quadratic term of this parabola is $-b_\epsilon^2$.

We are talking about "jumps" from one parabola to another, because, generally speaking, $\epsilon_{\mathrm{I}} \neq \epsilon_1$ and $\epsilon_{\mathrm{II}} \neq \epsilon_2$. The presence of jumps means that the relative existence time of the second mode ϵ_H does not vary from zero to unity with increasing void fractions in slug flows, but it has a non-zero minimum and a maximum which is less than 1. This effect can be observed in two-phase flow experiments when, for example, liquid bridging disappears if the length of the liquid slug decreases to a critical value; see Dukler & Taitel (1986). The location of the second parabola is not always symmetrical with respect to the $\epsilon = 0.5$ void fraction value. It is shifted toward higher void fractions if $\epsilon_2 > 1 - \epsilon_1$ and toward lower void fractions when $\epsilon_2 < 1 - \epsilon_1$.

The behavior of the variance of void fraction fluctuations in various two-phase flows and during flow regime transition will be analyzed in the next chapter based on calculations using the binomial model of bubble statistics.

3. DISCUSSION

Two methods will be used in this chapter. The first method is based on spectral analysis of artificially generated uni- and bimodal void fraction fluctuation signals which obey Bernoulli statistics. In the second method, parameter studies will be conducted by making use of the analytical expressions in [21] in order to describe the dependence of variance of void fraction fluctuations on various properties of two-phase flows.

3.1. Numerical simulation of periodic bimodal noise

Before introducing results of numerical simulations, an example of the biparabolic variance versus void fraction relation is shown in figure 1. The parameters of the model are: $\epsilon_1 = 0.15$, $\epsilon_2 = 0.65$, $\epsilon_{\rm I} = 0.2$, $\epsilon_{\rm II} = 0.6$, $b_0^2 = 1.25$, $b_\epsilon^2 = 6.25$. For the sake of simplicity, zero background noise level has been used; $\sigma_0 = 0$. In the region of void fractions with slug flow ($\epsilon_{\rm I} < \epsilon < \epsilon_{\rm II}$), periodic alteration of modes has been assumed with an oscillation frequency of 1.28 Hz. In figure 1, the solid line indicates the variance value evaluated according to [21]. One can see the "jumps" from one parabola to another at void fractions 0.2 and 0.6, which represent bubbly-to-slug and slug-to-annular flow regime transitions, respectively. The corresponding $\sigma_{\rm L_{max}}$ and $\sigma_{\rm L_{min}}$ values are 0.9 and 0.1. Dashed lines indicate two parabolas. The first parabola, which is less steep, belongs to unimodal flow. The second parabola is more steep and it represents bimodal flow regime. The bimodal parabola is steeper than the unimodal one because b_ϵ^2 is always larger than b_0^2. The ratio $b_\epsilon^2/b_0^2 = N = 5$ in this model. We chose this rather small value of the maximum number of bubbles in the observation volume in order to emphasize the presence of two parabolas. A small value of N corresponds, for example, to narrow-beam experiments with boiling in a tube of small diameter ($d \approx 1$ cm) under atmospheric pressure conditions. In the case of larger observation volume and/or higher pressure, N is much larger and the unimodal parabola is rather flat compared to the parabola which describes bimodal flows.

Spectral effects caused by periodic oscillations in bimodal two-phase flows have been studied by means of numerical simulation. Signals have been generated with a sampling time of 31.25 ms and

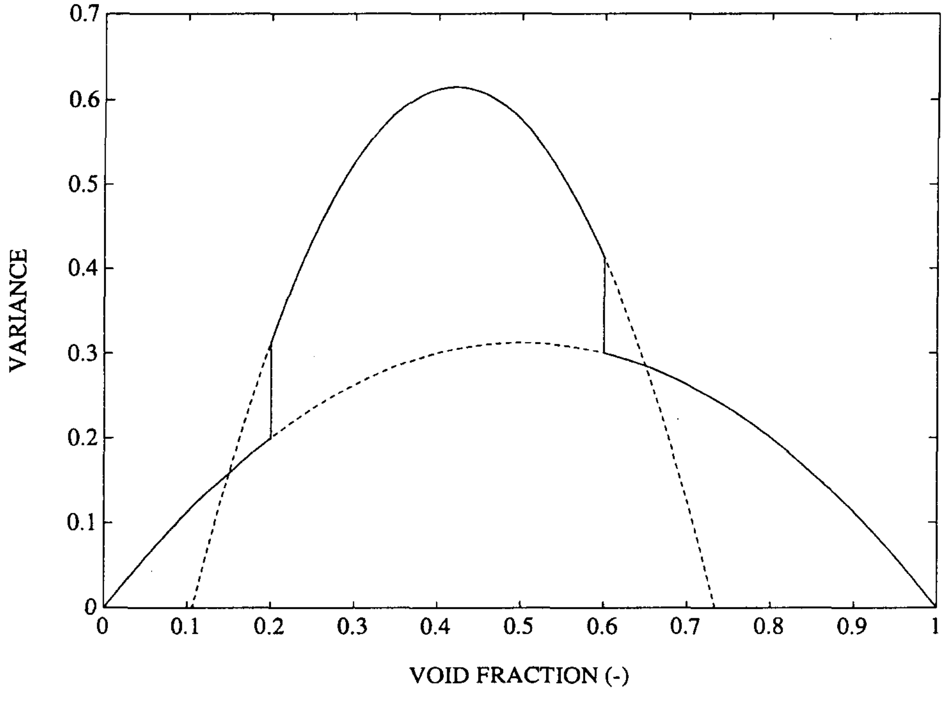

Figure 1. Variance of void fraction fluctuations as a function of the void fraction according to the binomial model; parameters of the model are: $\epsilon_1 = 1.15$, $\epsilon_2 = 0.65$, $\epsilon_{\rm I} = 0.2$, $\epsilon_{\rm II} = 0.6$. ——, Variances belonging to unimodal flow (flat parabola) and bimodal flow (steeper parabola).

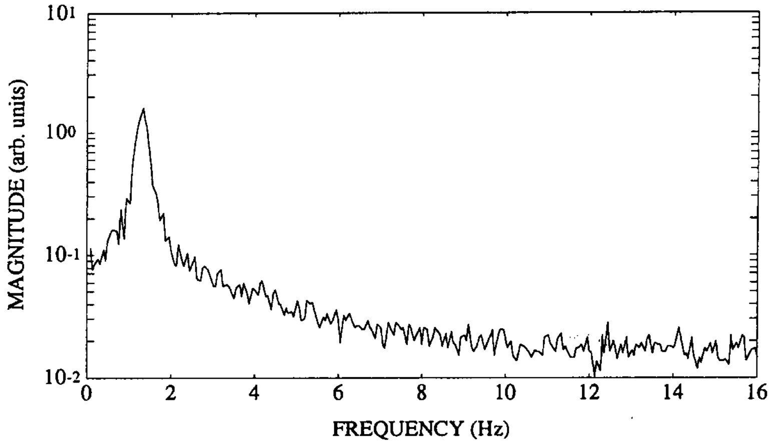

Figure 2. Magnitude of autospectrum of the simulated void fraction signal, $\epsilon = 0.37$. The oscillation peak is seen at 1.28 Hz.

with a block length of 512. The spectrum of the resulting bimodal signal have been evaluated by standard data analysis techniques; see Jenkins & Watts (1968). The fluctuation of the length of the liquid slug is also taken into account. Recently, several authors have analyzed the fractal nature of slug length; see Saether *et al.* (1990) and Nydal *et al.* (1992). In the present work, we use a very simple Gaussian model of slug length. The parameters of the model are L and σ_L, where L is the average slug length and $\sigma_L = \epsilon L$ is the standard deviation of L. In the calculations, a constant ϵ has been used: $\epsilon = 0.2$ (Saether *et al.* 1990).

The pdf does not depend on the way the modes are distributed in time. Therefore, the variance of the pdf remains unaffected by possible periodicities in the fluctuations. At the same time, the spectrum has a peak at frequency $f_0 = 1/(T_1 + T_2)$ and at its harmonics in the case of periodic alteration of modes. Here, T_1 and T_2 are the average residence times of the two modes. The spectral effect is illustrated in figure 2, where the autospectrum (APSD) of the simulated void fraction signal is shown for $\epsilon = 0.37$. This ϵ value corresponds to a variance value which is close to the maximum of the bimodal (steeper) parabola in figure 1. At frequencies much higher than f_0 the influence of periodic oscillations diminishes and the variances of the two modes determine the spectrum.

In the present analysis, the normalized band-passed variance of void fraction fluctuations σ_N^2 is used instead of NRMS^2. σ_N^2 is defined in a similar way as NRMS^2 in [2], the only difference is in the normalization factors. σ_N^2 is normalized by the square of signal level variation corresponding to 100% void. In the bimodal Bernoulli model, this quantity is denoted by b_ϵ^2, see [16]. NRMS^2 is normalized by I^2, the square of the total dc signal; see [2]. The proposed normalization for σ_N^2 might look complicated at first, but there is no serious difficulty in its practical implementation, as the effect of total voidage at the detector location is a directly measurable and/or computable quantity. The advantage of using σ_N^2 is that it contains quantitative information about the structure of the two-phase flow. This information will be analyzed in the next section.

The normalized band-passed variance of the spectrum has been determined over various frequency regions according to [2]. The results are depicted in figure 3 where the normalized band-passed variance is given as a function of the fractional existence time (ϵ_H) of the mode having the higher void fraction. The upper limit of the applied frequency band was always 16 Hz, while the lower limit was 0, 1, 2, 3 and 5 Hz for curves 1–5, respectively. The parameters of the model are the same as in figure 2, except for the background noise level ($\sigma_0 = 0.1$) and the maximum number of bubbles in the observation volume ($N = 100$). The first curve, which belongs to (0, 16 Hz), has the highest peak. The peaking of the curves is ceasing when the frequency region of the evaluation shifts towards higher frequencies. At frequencies much higher than $f_0 = 1/T = 1.28$ Hz, σ_N^2 is, in fact, independent of the oscillation between the modes, and it is the weighed sum of the variances of the two modes.

This result indicates that the high-frequency component of void fraction fluctuations changes monotonously with increasing void fractions even in the case of periodic oscillation of the modes,

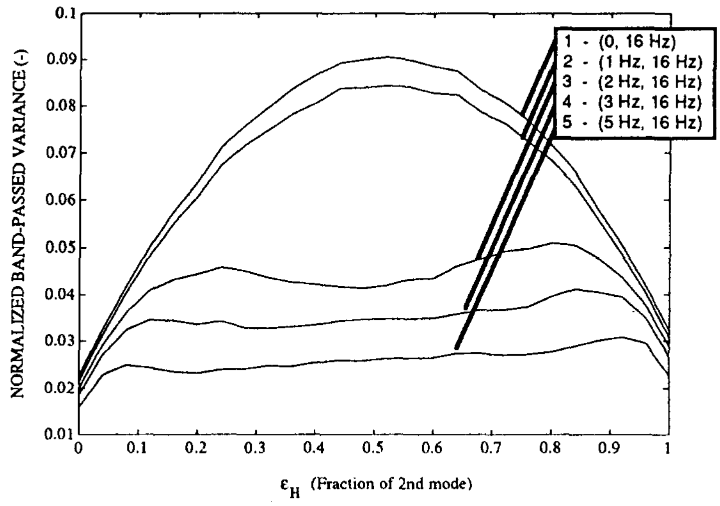

Figure 3. Calculated normalized band-passed variance as a function of ϵ_H and frequency band. The upper frequency is always 16 Hz; the lower frequencies are: 0, 1, 2, 3 and 5 Hz, respectively.

although, the full-range variance has a prominent maximum over the same range of void fraction variations. This observation is supported by the data in figure 4, where the effect of simultaneously changing frequency band and ϵ_H is shown in a three-dimensional plot. Note that ϵ_H does not vary beyond the limited range of 0.1–0.9 in actual bimodal flows. Within these limits, σ_N^2 is indeed a monotonous function of ϵ_H.

3.2. Determining the parameters of bubble populations

The typical size of bubbles has a profound impact on the intensity of void fraction fluctuations. Intuitively it is clear that the fluctuations are smaller if the void is dispersed in a lot of small bubbles, compared to the case when the same amount of void is concentrated in a few large bubbles.

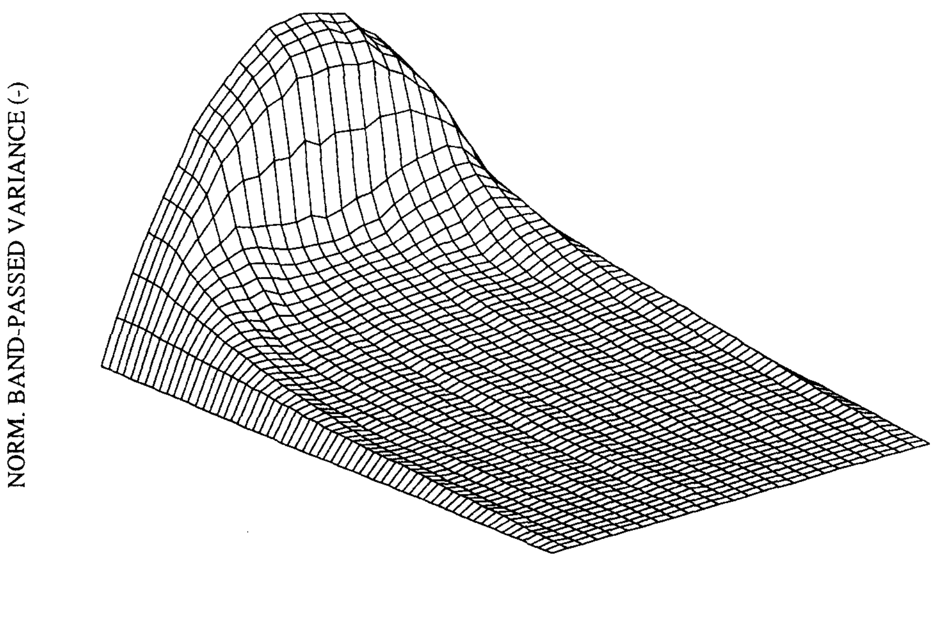

Figure 4. Three-dimensional plot of the dependence of band-passed variance on the frequency band and ϵ_H. Frequency varies from 0 to 16 Hz; ϵ_H varies between 0 and 1.

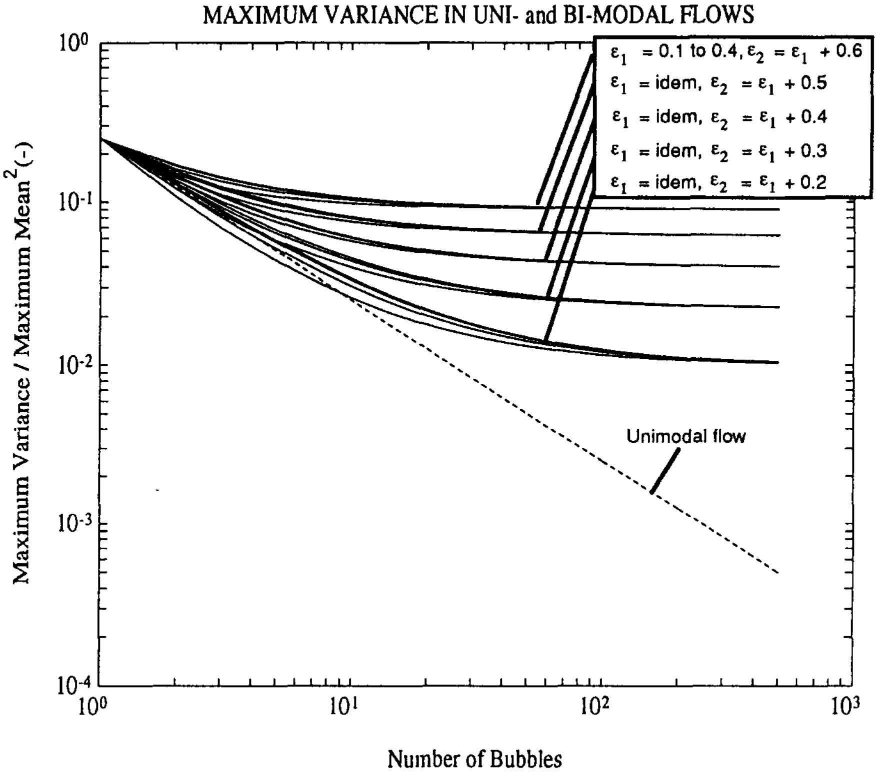

Figure 5. Maximum of normalized variance as the function of number of bubbles (N) and void fractions of the modes, ϵ_1 and ϵ_2, calculations with Na = const.

Quantitative characterization of this effect is given below based on the binomial model of uni- and bimodal flows.

First, consider the case of a fixed observation volume with $b_\epsilon = Na$ = const. If the average size of bubbles decreases, the constant observation volume can accommodate, on average, more bubbles. Therefore, N increases and a decreases. This situation can occur, for example, in an experiment with changing system pressure. The effect of changing N is illustrated in figure 5, based on the numerical evaluation of [21]. For the sake of clarity, only the maximum of the normalized variance is shown in figure 5. The position of the maximum is $\epsilon = 0.5$ in the case of unimodal flow, and it is determined by [12] in bimodal flows.

These maxima give a good indication about the changes in σ_N^2 generated by boiling. All the curves have a maximum value of 0.25 at $N = 1$ and decrease with increasing N. The decreasing tendency is the fastest for unimodal flows. In the case of $N = 100$ in unimodal flow, σ_N^2 is close to 10^{-3}. Based on the known value of N and on the actual level of background noise, the detectability of the onset of boiling in a given experimental arrangement can be evaluated. The situation becomes more complicated in the case of bimodal flows due to the larger number of free parameters. Nevertheless, it can be concluded that σ_N^2 reaches saturation between $N = 10$ and 100. The value of σ_N^2 at N values above 100 depends mainly on the difference of the void fractions of the modes. In all cases, the number of bubbles can be determined by fitting the experimentally determined σ_N^2 versus ϵ_H curve.

In figure 6, results of parameter studies are given in the case of constant average bubbles size, a = constant. This can be interpreted as the case of constant properties of two-phase flows, while the sensitivity volume of the detector changes. Such an effect can be observed when comparing measurement results obtained by different types of detectors or by changing the focusing of the beam in transmission methods, etc. All the curves increase monotonously with increasing N. Above about $N = 100$, σ_N^2 is determined mainly by the difference between the properties of the modes.

In the framework of the present study, we had the limited scope of performing parameter studies in order to illustrate the relationships between two-phase flow parameters and the statistical characteristics of void fraction fluctuations. Our results offer the possibility to obtain additional information about the structure of two-phase flows when applying the introduced binomial bubble fluctuation theory to the interpretation of actual experiments.

4. CONCLUSIONS

(1) Void fraction fluctuations in two-phase flows have been modeled by making use of binomial statistics of bubble dynamics. In the framework of this model, a general expression has been derived for the variance of void fraction fluctuations in various two-phase flow regimes, including bubbly-to-slug and slug-to-annular flow transitions. It has been shown that the dependence of the variance on the void fraction can be described by means of two parabolic relationships. The first parabola is rather flat and it describes fluctuations in unimodal flows. The second one belongs to bimodal flows and it is usually much steeper than the first one. Flow regime transitions in two-phase flows have been modeled as "jumps" from one parabola to the other.

(2) The frequency-content of void fraction fluctuations has been studied by means of band-passed noise intensity. Periodic bimodal void fraction fluctuations in slug flows have been analyzed with the help of numerical simulations. Based on this analysis, we have explained why the high-frequency component of void fraction fluctuations changes monotonously with increasing void fractions, while the total variance has a prominent maximum over the same range of void fraction variations. It is shown that the high-frequency component of the variance is, in fact, independent of the oscillations between the modes and it is the weighted sum of the variances of the two modes.

(3) Perhaps the most important consequence of the biparabolic model is that it allows us to estimate the average size and number of bubbles seen by the detector via monitoring the magnitude of normalized variance of void fraction fluctuations. We developed a method to

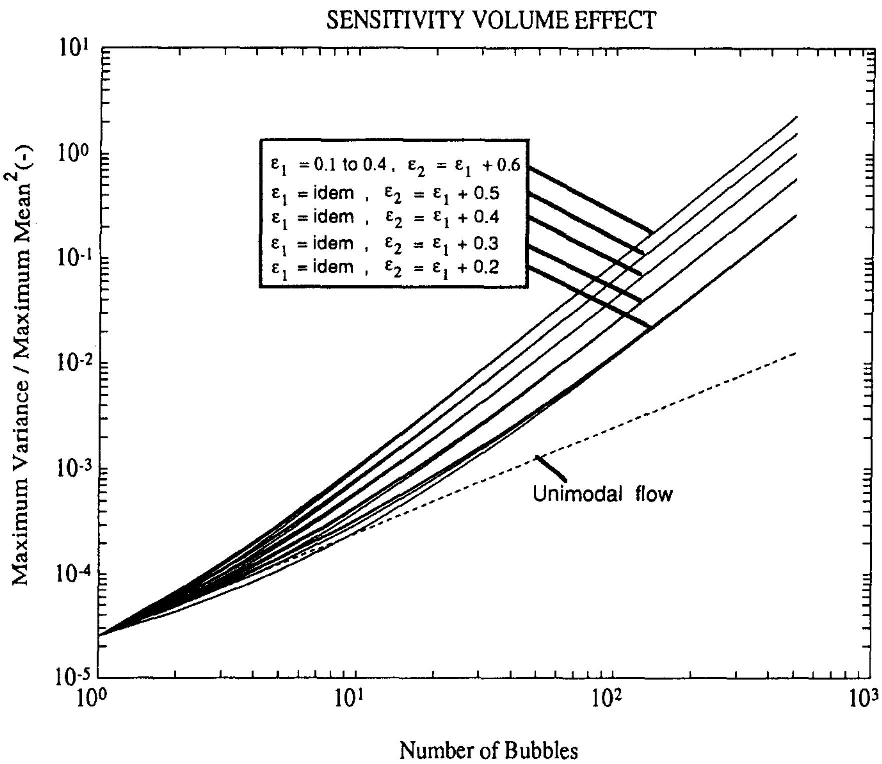

Figure 6. Maximum of normalized variance as the function of number of bubbles (N) and void fractions of the modes, ϵ_1 and ϵ_2; the case of a = const.—changing sensitivity volume effect.

determine the number of bubbles in the sensitivity volume of the detector based on biparabolic fit of the measured void fraction versus variance of void fractions relationship. By applying the present theoretical results to the interpretation of measurements, a better insight can be gained about the complex processes in two-phase flows.

REFERENCES

ALBRECHT, R. W. CROWE, R. D. DAILEY, D. J. & HOLLENBACH, D. F. 1984 Neutronic fluctuation analysis as a characterizing vehicle for two-phase flow. In *Measuring Techniques in Gas–Liquid Two-phase Flows* (Edited by DELHAYE, J. M. & COGNET, G.), pp. 337–358. Springer, Berlin.

DUKLER, A. E. & TAITEL, Y. 1986 Flow pattern transitions in gas–liquid systems: measurement and modeling. *Multiphase Sci. Technol.* **2,** 1–94.

FRANCA, F., ACIKGOZ, M., LAHEY, R. T. JR & CLAUSSE, A. 1991 The use of fractal techniques for flow regime identification. *Int. J. Multiphase Flow* **17,** 545–552.

GAERTNER, R. F. 1965 Photographic study of nucleate pool boiling on a horizontal surface. *J. Heat Transfer Trans. ASME* **87,** 17–29.

GOVIER, G. W. & AZIZ, K. 1972 *The Flow of Complex Mixtures in Pipes.* Van Nostrand Reinhold, New York.

JAIN, P. K. & ROY, R. P. 1983 Stochastic characteristics of vapor fraction and wall pressure fluctuations in boiling flows. *Int. J. Multiphase Flow* **9,** 463–489.

JENKINS, G. M. & WATTS, D. G. 1968 *Spectral Analysis and its Applications.* Holden Day, San Francisco, CA.

JONES, O. C. & ZUBER, N. 1975 The interrelation between void fraction fluctuations and flow patterns in two-phase flow. *Int. J. Multiphase Flow* **2,** 273–306.

LAHEY, R. T. JR, KRYCUK, G. & MALAVIYA, B. K. (1978) A high-intensity X-ray system for stochastic measurements of two-phase flows. *Trans. ANS* **30,** 497–499.

LIN, P. Y. & HANRATTY, T. J. 1987 Detection of slug flow from pressure measurements. *Int. J. Multiphase Flow* **13,** 13–21.

LUBBESMEYER, D. & LEONI, B. (1983) Fluid velocity measurements and flow-pattern identification by noise-analysis of light-beam signals. *Int. J. Multiphase Flow* **9,** 665–679.

MATSUI, G. 1986 Automatic identification of flow regimes in vertical two-phase flow using differential pressure fluctuations. *Nucl. Engng Des.* **95,** 221–231.

MATUSZKIEWICZ A., FLAMAND, J. C. & BOURE, J. A. 1987 The bubble-slug flow pattern transition and instabilities of void fraction waves. *Int. J. Multiphase Flow* **13,** 199–217.

MCQUILLAN, K. W. & WHALLEY P. B. 1985 Flow patterns in vertical two-phase flows. *Int. J. Multiphase Flow* **11,** 161–175.

NYDAL, O. J., PINTUS, S. & ANDREUSSI, P. (1992) Statistical characterization of slug flow in horizontal pipes. *Int. J. Multiphase Flow* **18,** 439–453.

OHLMER, E., FORTESCUE, T., RIEBOLD, W., BORS, B., IMMINK, J., & WESSER, U. 1984 Two-phase flow identification by calibration with stochastic parameters. In *Measuring Techniques in Gas–Liquid Two-phase Flows* (Edited by DELHAYE, J. M. C., COGNET, G.), pp. 563–585. Springer, Berlin.

SAETHER, G., BENDIKSEN, K., MULLER, J. & FROLAND, E. 1990 The fractal statistics of liquid slug lengths. *Int. J. Multiphase Flow* **16,** 1116–1126.

SULTAN, M. & JUDD, R. L. 1978 Spatial distribution on active bubble sites and bubble flux density. *Trans. ASME* **100,** 56–62.

TAITEL, T., BARNEA, D. & DUKLER, A. E. 1980 Modeling flow pattern transitions for steady upward gas–liquid flow in vertical tubes. *AIChE Jl* **26,** 345–354.

TUTU, N. K. 1984 Pressure drop fluctuations and bubble-slug transition in a vertical two-phase water flow. *Int. J. Multiphase Flow* **10,** 211–216.

VINCE, M. A. & LAHEY, R. T. Jr (1982) On the development of an objective flow regime indicator. *Int. J. Multiphase Flow* **8,** 93–124.